MIT Libraries | DSpace@MIT

MIT Open Access Articles

Identification of CDCP1 as a hypoxia-inducible factor 2 (HIF-2) target gene that is associated with survival in clear cell renal cell carcinoma patients

The MIT Faculty has made this article openly available. ***Please share*** how this access benefits you. Your story matters.

Citation: Emerling, B. M., C. H. Benes, G. Poulogiannis, E. L. Bell, K. Courtney, H. Liu, R. Choo-Wing, et al. "Identification of CDCP1 as a hypoxia-inducible factor 2 (HIF-2) target gene that is associated with survival in clear cell renal cell carcinoma patients." Proceedings of the National Academy of Sciences 110, no. 9 (February 26, 2013): 3483-3488.

As Published: http://dx.doi.org/10.1073/pnas.1222435110

Publisher: National Academy of Sciences (U.S.)

Persistent URL: http://hdl.handle.net/1721.1/80378

Version: Final published version: final published article, as it appeared in a journal, conference proceedings, or other formally published context

Terms of Use: Article is made available in accordance with the publisher's policy and may be subject to US copyright law. Please refer to the publisher's site for terms of use.

Massachusetts Institute of Technology

Identification of CDCP1 as a hypoxia-inducible factor 2α (HIF-2α) target gene that is associated with survival in clear cell renal cell carcinoma patients

Brooke M. Emerling[a,b], Cyril H. Benes[c,d], George Poulogiannis[a,b], Eric L. Bell[e], Kevin Courtney[f,g], Hui Liu[a,b], Rayman Choo-Wing[a,b], Gary Bellinger[a,b], Kazumi S. Tsukazawa[a,b], Victoria Brown[f,h], Sabina Signoretti[f,h], Stephen P. Soltoff[b], and Lewis C. Cantley[a,b,1]

[a]Department of Systems Biology, Harvard Medical School, Boston, MA 02115; [b]Division of Signal Transduction, Beth Israel Deaconess Medical Center, Boston, MA 02115; [c]Massachusetts General Hospital Cancer Center, Charlestown, MA 02129; [d]Department of Medicine, Harvard Medical School, Boston, MA 02115; [e]Paul F. Glenn Laboratory, Department of Biology, Massachusetts Institute of Technology, Cambridge, MA 02139; [f]Department of Medical Oncology, Dana-Farber Cancer Institute, Boston, MA 02115; [g]Division of Hematology-Oncology, University of Texas Southwestern Medical Center, Dallas, TX; and [h]Department of Pathology, Brigham and Women's Hospital, Harvard Medical School, Boston, MA 02115

Contributed by Lewis C. Cantley, December 28, 2012 (sent for review June 20, 2012)

CUB domain-containing protein 1 (CDCP1) is a transmembrane protein that is highly expressed in stem cells and frequently overexpressed and tyrosine-phosphorylated in cancer. CDCP1 promotes cancer cell metastasis. However, the mechanisms that regulate CDCP1 are not well-defined. Here we show that hypoxia induces CDCP1 expression and tyrosine phosphorylation in hypoxia-inducible factor (HIF)-2α–, but not HIF-1α–, dependent fashion. shRNA knockdown of CDCP1 impairs cancer cell migration under hypoxic conditions, whereas overexpression of HIF-2α promotes the growth of tumor xenografts in association with enhanced CDCP1 expression and tyrosine phosphorylation. Immunohistochemistry analysis of tissue microarray samples from tumors of patients with clear cell renal cell carcinoma shows that increased CDCP1 expression correlates with decreased overall survival. Together, these data support a critical role for CDCP1 as a unique HIF-2α target gene involved in the regulation of cancer metastasis, and suggest that CDCP1 is a biomarker and potential therapeutic target for metastatic cancers.

kidney cancer | oxygen deprivation

CUB domain-containing protein 1 (CDCP1), also known as transmembrane and associated with SRC kinase (TRASK) and subtractive immunization M^+ HEp3-associated 135-kDa protein (SIMA135), is a substrate and binding protein for the Src-family tyrosine kinases (SFKs). CDCP1 is overexpressed and highly tyrosine-phosphorylated in multiple cancers (1, 2), predominantly renal (3, 4), breast (2), colon (2, 5, 6), pancreatic (7), and lung cancers (2). At present, the functional importance of CDCP1 has been reported in patients with metastatic carcinomas as well as in a number of epithelial cancer cell lines (3, 6, 8–14). However, mechanisms regulating CDCP1 are not well-defined. Studies from our laboratory revealed a biochemical pathway by which CDCP1 participates in the activation of Src-family members and the coupling of SFK activation to phosphorylation and regulation of protein kinase C delta (PKC-δ) (15).

Importantly, a recent study shows that CDCP1 plays a critical role in the process of metastasis and in the survival of cells at distant sites of metastasis (16). Here we demonstrate a unique role for CDCP1 under conditions of oxygen deprivation (hypoxia).

Hypoxia triggers the elevation of hypoxia-inducible factors HIF-1α and HIF-2α by blocking von Hippel Lindau (VHL)-dependent HIF-α degradation (17–19). HIF is a heterodimer of two basic helix-loop-helix/PAS proteins, HIF-α and the aryl hydrocarbon nuclear translocator (ARNT or HIF-β) (20). HIF-α and ARNT subunits are ubiquitously expressed; however, the α-subunit is labile under conditions of normal oxygen (5–21% O_2). Under hypoxic conditions (0.5–5% O_2) the HIF-α subunit is stabilized, dimerizes with ARNT, translocates to the nucleus, and subsequently binds to hypoxia response elements (HREs) within target genes. Among HIF transcription targets are genes involved in glucose metabolism, angiogenesis, and metastasis (21), thereby tightly linking HIF-mediated transcription to tumorigenesis (22). HIF-1α and HIF-2α are overexpressed in a number of primary and metastatic human cancers. HIF-1α and HIF-2α play particularly critical, and opposing, roles in clear cell renal cell carcinoma (ccRCC), where VHL loss is a frequent event. HIF-2α, but not HIF-1α, can abrogate the tumor suppressor function of VHL, and HIF-2α inhibition impairs growth of VHL-null RCCs (23–27). Conversely, HIF-1α appears to play a tumor suppressor role in kidney cancer (28). These results are surprising, because most of the genes regulated by HIF-2α are also regulated by HIF-1α. Consequently, identification of genes that exhibit differential transcriptional regulation by HIF-1α and HIF-2α would enhance our understanding of the mechanisms underlying the pathogenesis of ccRCC.

Results

In the course of evaluating the effect of hypoxia on the growth and survival of transformed and nontransformed cells, we discovered that hypoxia caused a dramatic increase in protein expression and tyrosine phosphorylation of CDCP1 (Fig. 1*A*). Full-length CDCP1 is 135 kDa and is posttranslationally processed in a range of cell lines by a mechanism involving serine protease activity, thereby generating a C-terminal 70-kDa fragment (29). In the human colorectal carcinoma cell lines HCT116 and DLD1, both fragments of CDCP1 are tyrosine-phosphorylated when exposed to hypoxia or the hypoxia mimetic deferoxamine (DFO), an iron-chelating agent (Fig. 1). Importantly, exposure to hypoxia enhances CDCP1 phosphorylation at tyrosine 734, and this correlates with the activation of Src (Fig. 1*B*). Tyrosine 734 is a Src SH2 binding site (15) and is required for CDCP1-mediated lung metastasis (16). [Characterizations of the phospho-site specificity of the Tyr-P-734 antibody have been previously described (30).] Interestingly, CDCP1 tends to target Src to specific substrates (CDCP1, PKC-δ, SHC), and thus phosphorylation of Y734 of CDCP1 (an established Src-family site) provides evidence of local Src activity. Additionally, Src inhibition by dasatinib diminishes CDCP1 tyrosine phosphorylation induced by DFO (Fig. 1*C*).

Author contributions: B.M.E. and C.H.B. designed research; B.M.E., C.H.B., G.P., E.L.B., K.C., H.L., R.C.-W., G.B., K.S.T., V.B., and S.S. performed research; B.M.E., C.H.B., E.L.B., K.C., S.S., S.P.S., and L.C.C. analyzed data; and B.M.E. wrote the paper.

The authors declare no conflict of interest.

[1]To whom correspondence should be addressed. E-mail: lewis_cantley@hms.harvard.edu.

This article contains supporting information online at www.pnas.org/lookup/suppl/doi:10.1073/pnas.1222435110/-/DCSupplemental.

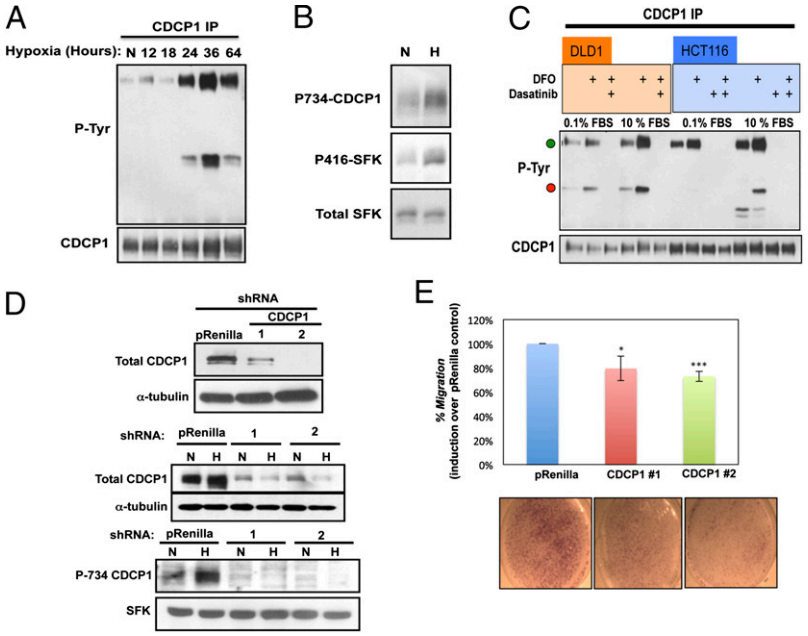

Fig. 1. Hypoxia activates the CDCP1-Src pathway. (*A*) HCT116 cells were exposed to 21% O_2 (normoxia; N) or 1% O_2 (hypoxia; H) for 12, 18, 24, 36, or 64 h. The anti-CDCP1 antibody was used for immunoprecipitation (IP) and immunoblotting. An anti-phosphotyrosine antibody was used for immunoblotting. (*B*) HCT116 cells were exposed to N or H for 48 h. Lysates were immunoblotted for the phosphorylation of CDCP1 and Src-family kinases using a specific CDCP1 P-734 antibody that recognizes CDCP1 when phosphorylated on Tyr734 and a P-416 SFK antibody that recognizes the activation loop of Src-family kinases when phosphorylated at Tyr416. An anti-SFK antibody was used as loading control. (*C*) DLD1 and HCT116 cells cultured in 0.1% or 10% FBS were treated ±100 μM DFO and/or 50 nM dasatinib for 24 h. The anti-CDCP1 antibody was used for immunoprecipitation and immunoblotting. An anti-phosphotyrosine antibody was used for immunoblotting. (*D*) Two retroviral shRNAs targeted against CDCP1 were used to stably knock down CDCP1 in MCF10A cells. An anti-tubulin antibody was used as loading control. Stable cell lines were exposed to N or H for 48 h. Lysates were immunoblotted for the phosphorylation of CDCP1 and SFKs as in *B* using the specific CDCP1 P-734 antibody and the anti-SFK antibody for loading control. (*E*) Stable CDCP1 knockdown MCF10A cell lines were serum-starved and exposed to 1% O_2 for 24 h; subsequently, the cells were seeded in transwells and returned to 1% O_2 for 24 h. Cells were fixed and stained with crystal violet (0.1%; *Lower*). The number of cells that migrated to the bottom of the filter was counted and the data are reported as fold induction over the pRenilla control cells. The data presented are the result of triplicate analyses and the error bars indicate SEM. *$P = 0.088$, ***$P = 0.0007$.

To evaluate the role of CDCP1 in cellular responses to hypoxia, we used two different retroviral shRNAs targeted against CDCP1 providing significant knockdown in an immortalized human mammary epithelial cell line (MCF10A; Fig. 1*D*). As expected, stable CDCP1 knockdown resulted in reduced hypoxia-induced tyrosine phosphorylation of CDCP1 (Fig. 1*D*). Moreover, the reduction of CDCP1 phosphorylation correlated with reduced phosphorylation of SFK (Fig. 1*D*), consistent with CDCP1 playing a critical role in hypoxia-induced activation of SFKs. Importantly, in keeping with the role of CDCP1 and SFKs in migration (4, 30), knocking down CDCP1 reduced migration of MCF10A cells under conditions of hypoxia (Fig. 1*E*), without having any affect on cell proliferation. Together, these data show that hypoxia activates a CDCP1-Src signaling pathway that appears to play a critical role in migration under hypoxic conditions.

HIF is the key transcription factor that regulates cellular responses to hypoxia. To determine whether HIF regulates CDCP1, we generated stable cell lines using the lentiviral pLK0.1 system. MCF10A cells were generated that stably express shRNAs targeting HIF-1α, HIF-2α, or ARNT (Fig. 2*A*). Remarkably, knockdown of HIF-2α with two different independent hairpins, but not HIF-1α, impaired hypoxia-induced CDCP1 expression and tyrosine phosphorylation, as well as SFK activation (Fig. 2 *B* and *C* and Fig. S1). As expected, knockdown of ARNT, which is required for both HIF-1α and HIF-2α function, also prevented the hypoxic activation of CDCP1. Quantitative real-time PCR (qRT-PCR) was used to demonstrate that *Cdcp1* mRNA level increased under hypoxia in a HIF-2α–dependent manner. Hypoxia induced a dramatic increase in *Cdcp1* mRNA level in the pLK0.1 vector and GFP control lines, as well as in the HIF-1α knockdown line, but not in the HIF-2α and ARNT knockdown lines (Fig. 2*C*). In addition, chromatin immunoprecipitation (ChIP) demonstrated an increase in binding of HIF-2α and ARNT but not of HIF-1α to the CDCP1 promoter in response to hypoxia (Fig. 2*D*). These results indicate that the HIF-2α–ARNT complex directly regulates *Cdcp1* expression. An HRE/ARNT binding site was identified within the promoter of CDCP1 (Fig. 2*E*) ~2 kb upstream from the transcription start site. We cloned the genomic region surrounding the predicted HIF binding site within the CDCP1 promoter into a luciferase reporter construct and showed that the hypoxic mimetics DFO and dimethyloxaloylglycine (DMOG) activate the CDCP1 promoter reporter in comparison with the scrambled control promoter (Fig. 2*F*). Knocking down CDCP1 impaired migration under hypoxia and notably the knockdown of HIF-2α reduced migration, whereas the knockdown of HIF-1α showed no effect on migration (Fig. 2*G*). Importantly, CUB1, an antibody against the extracellular domain of CDCP1 that activates Src-family kinases and induces Tyr phosphorylation of CDCP1 (30), rescued the migration defect of the HIF-2α knockdown line (Fig. 2*G*). Together, these results show that CDCP1 is a HIF-2α–specific target gene that enhances migration in response to hypoxia.

To determine whether HIF-2α promotes CDCP1 expression and tyrosine phosphorylation in vivo, we introduced a doxycycline-inducible form of HIF-2α into A375 melanoma cells and compared CDCP1 levels in these cells with CDCP1 levels in A375 cells expressing GFP using murine xenografts. To circumvent the degradation of HIF-2α by VHL, we mutated the two Pro residues, whose hydroxylation mediates degradation (31, 32), to Ala (HIF-2α P405A; P531A, or HIF-2αDPA, double-

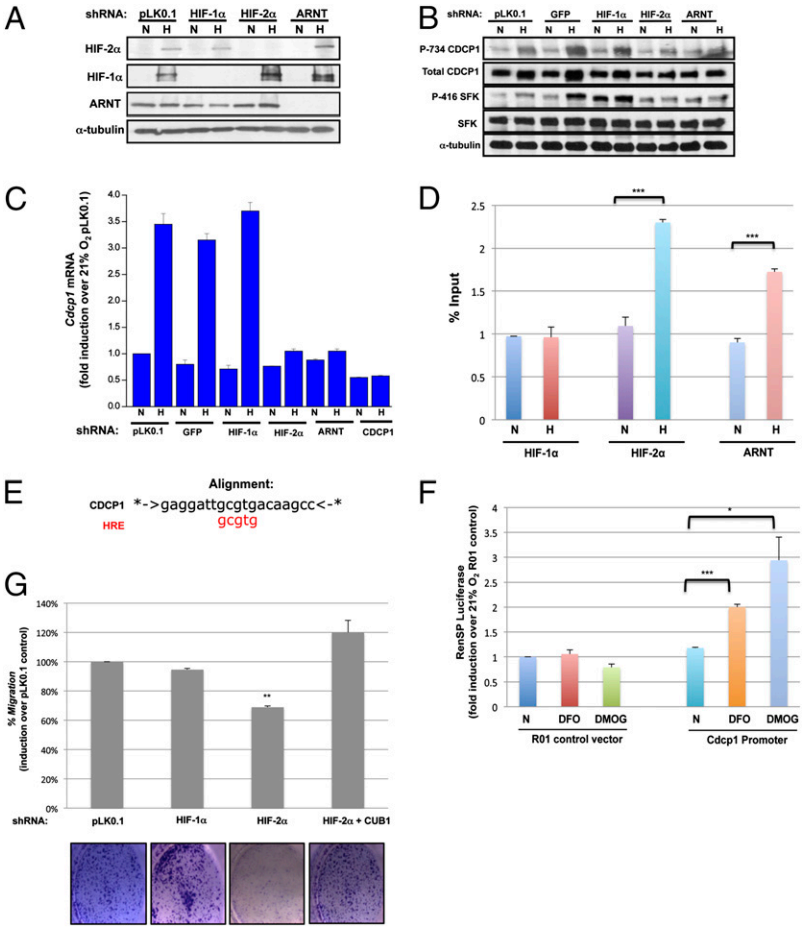

Fig. 2. Hypoxic activation of CDCP1 is HIF-2α–dependent. (*A*) Stable knockdown of HIF-1α, HIF-2α, and ARNT in MCF10A cells. (*B*) Stable cell lines exposed to 21% O_2 (N) or 1% O_2 (H) for 48 h. Lysates were immunoblotted for CDCP1, P-734 CDCP1, P-416 SFK, SFK, and α-tubulin for loading control. (*C*) Quantitative real-time PCR for *Cdcp1* on mRNA isolated from MCF10A stable cell lines cultured in N or H for 24 h. Data are represented as the means ± SEM ($n = 3$). (*D*) MCF10A cells were exposed to N or H for 24 h and subsequently ChIP was carried out on DNA–protein complexes with anti–HIF-1α, anti–HIF-2α, anti-ARNT, or control IgG antibodies followed by qRT-PCR. Antibodies used are indicated on the *x* axis. Data are represented as the means ± SEM ($n = 3$). ***$P < 0.0001$, two-tailed Student's *t* test. (*E*) Alignment of *Cdcp1* (chromosome 3) with the predicted HRE/ARNT binding site using MAPPER2 (http://genome.ufl.edu/mapper). Red indicates the predicted HRE/ARNT binding site. (*F*) HT1080 cells were transfected with the R01-scrambled control vector or with the Cdcp1-promoter vector. At 24 h after transfection, cells were exposed to 21%O_2 (N) ±100 μM DFO or 1 mM DMOG. RenSP luciferase was measured and the data are reported as fold induction over untreated normoxic R01 control vector cells. The data presented are the result of triplicate analyses and the error bars represent SEM. *$P = 0.02$, ***$P = 0.0002$. (*G*) Stable MCF10A cell lines were serum-starved and exposed to 1% O_2 for 24 h; subsequently, the cells were seeded in transwells and returned to 1% O_2 for 24 h. CUB1 mAb was added at the time of seeding to the top and bottom chambers. Cells were fixed and stained with crystal violet (0.1%; *Lower*). The number of cells that migrated to the bottom of the filter was counted and the data are reported as fold induction over the pLK0.1 control cells. The data presented are the result of triplicate analyses and the error bars indicate SEM. **$P < 0.001$, two-tailed Student's *t* test.

proline to alanine). Endogenous HIF-2α levels are very low in the A375 cell line, and overexpression of HIF-2α is known to be a promoter of tumor growth (24, 26). Consistent with previous findings, A375 cells expressing HIF-2αDPA formed larger and more vascularized tumors in nude mice compared with the GFP control-expressing cells (Fig. 3 *A* and *B*). In addition, induction of HIF-2α expression by doxycycline was sufficient to induce protein expression and tyrosine phosphorylation of CDCP1 in vivo (Fig. 3*C* and Fig. S2). Moreover, the overexpression of HIF-2α significantly enhanced lung metastases in NOD/SCID mice (Fig. 3*D*).

To investigate the relationship between HIF-2α and CDCP1 expression, we performed a correlation analysis in the largest up-to-date collection (Sanger Cell Line Project) of cancer cell line microarray data ($n = 732$). We found a dramatic concordance in the expression of HIF-2α and CDCP1 (Pearson's correlation, $P = 1 \times 10^{-20}$), indicating that cancers with high HIF-2α expression tend to have high levels of CDCP1 expression (Fig. 3*E*). We next asked whether other known HIF-2α target genes also correlate in this expression analysis. Remarkably, Met proto-oncogene hepatocyte growth factor receptor (MET) and epidermal growth factor receptor (EGFR), which are hypoxia-regulated and known HIF-2α target genes, also displayed a strong correlation with HIF-2α and CDCP1 expression (Fig. 3 *F* and *G*).

To further examine CDCP1 expression in cancer, we performed a comprehensive analysis of CDCP1 expression across multiple tumor types and found that the abundance of *Cdcp1* message is significantly increased in many cancers compared with their corresponding normal tissue. The most dramatic expression differences were seen in bladder, breast, colorectal, kidney, ovarian, and pancreatic carcinomas (Fig. S3*A*). Next, we identified a colon cancer dataset where high CDCP1 expression was associated with poorer prognosis markers, such as recurrence in 5 y (Fig. S3*B*). Similarly, analysis of a large dataset of lung adenocarcinomas (>400) demonstrated a strong statistical association between higher CDCP1 expression and shorter patient survival (Fig. S3*C*). Finally, we found that CDCP1 tyrosine phosphorylation is significantly higher in triple-negative breast cancer cell lines (Fig. S3*D*), and triple-negative breast cancers have poor outcomes in the metastatic setting. Thus, across multiple cancer types, a higher level of CDCP1 expression is found to correlate with poorer prognosis, possibly related to a higher propensity of metastasis.

The results suggest that therapeutic approaches targeting CDCP1, such as monoclonal antibodies, could be beneficial in cancers that exhibit high levels of HIF-2α and other features of hypoxia. This might be particularly relevant in ccRCC, where hypoxia-regulated pathways play a critical role, and which responds poorly to treatment with cytotoxic chemotherapy and ranks among the most radio- and chemoresistant cancers. Although surgery is the treatment of choice for patients diagnosed with early stages of ccRCC, greater than 30% of patients are diagnosed with metastatic ccRCC, and a large fraction of these patients develop metastases after surgery.

Previous studies have shown that high CDCP1 can be correlated with low overall patient survival in kidney cancer (1–4). As HIF-2α regulates CDCP1 expression and is a critical driver of ccRCC, we examined a kidney cancer tissue array containing samples from 63 patients with conventional ccRCC for CDCP1 expression by immunohistochemistry (IHC) (Fig. 4 *A* and *B*). The tissue array contained samples from patients with both localized and metastatic disease. Kaplan–Meier analysis from the date of diagnosis reveals that high CDCP1 immunohistochemical

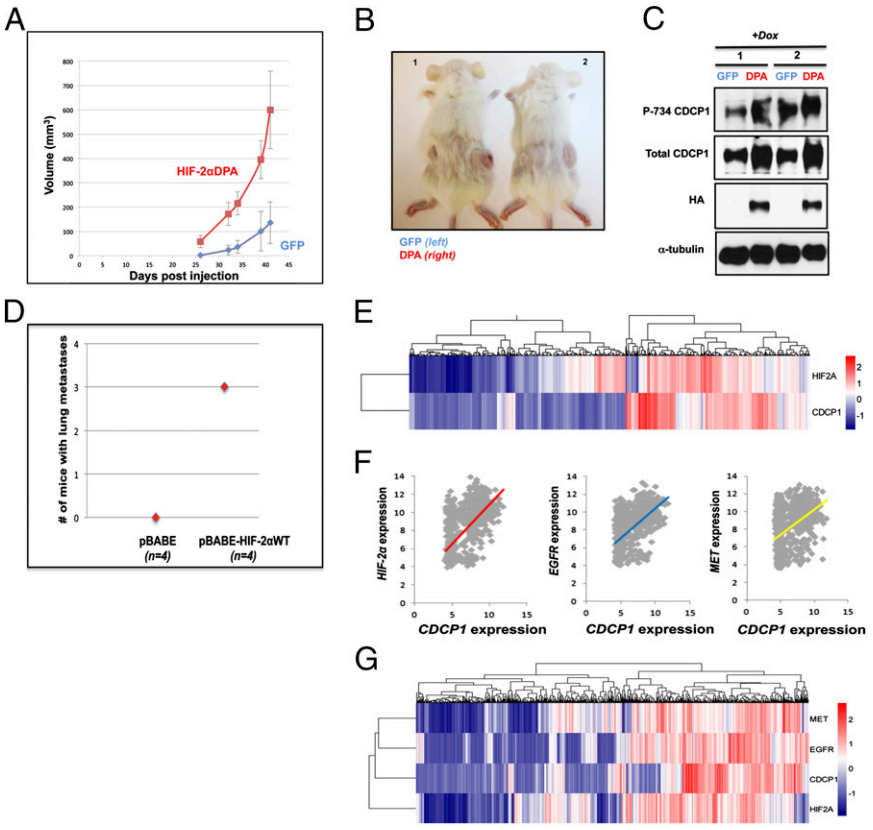

Fig. 3. HIF-2α is sufficient to activate CDCP1 and promote tumor growth in xenografts. (*A*) Tumor formation over time in nude mice injected with the A375 cancer cell line expressing GFP or HIF-2αDPA. Doxycycline chow was used to induce expression of GFP or HIF-2αDPA. Error bars are SEM. (n = 6). (*B*) Representative images of tumors; GFP control cells (left flank) or HIF-2αDPA (right flank) after mice were euthanized. (*C*) Protein was isolated from tumors and immunoblotted for CDCP1, P-734 CDCP1, HA, and α-tubulin for loading control. Shown are two representative tumors from the mice. (*D*) Scatterplot shows that overexpression of HIF-2α significantly enhanced lung metastases in NOD/SCID mice. The number of mice with surface lung metastases was counted 9 wk after tail-vein injections (n = 4). (*E*) Heat map of CDCP1 and HIF-2α expression based on the microarray data of 732 unique cancer cell lines from the SCLP. (*F*) Scatterplots comparing the expression levels of CDCP1 with HIF-2α (*Left*), EGFR (*Center*), and MET (*Right*), all showing a strong positive correlation in their expression across the 732 cancer cell lines ($P = 1 \times 10^{-20}$, Pearson's correlation coefficient analysis). (*G*) Heat map of CDCP1, HIF-2α, EGFR, and MET expression across the SCLP (n = 732).

staining correlates with poor overall survival (Fig. 4*C*). Interestingly, high-grade ccRCCs (G3, G4) expressed significantly higher (P = 0.03, t test) levels of CDCP1 protein compared with lower-grade tumors (G1, G2), suggesting that CDCP1 expression increases progressively with higher ccRCC tumor grade. In keeping with these results, VHL-deficient RCC cell lines (some of which express HIF-2α, but not HIF-1α) express high CDCP1 protein levels, and display high CDCP1 tyrosine phosphorylation under normal oxygen conditions (Fig. 4*D*). These results suggest that CDCP1 is a potential biomarker and therapeutic target for ccRCC.

Discussion

Here we found that HIF-2α, but not HIF-1α, is essential for induction of CDCP1 expression in response to hypoxia. Although hypoxia induced the expression of CDCP1, the mechanism leading to the tyrosine phosphorylation of CDCP1 is not fully understood, and it is possible that hypoxia induces the expression of an unidentified ligand for CDCP1. More broadly, these data support a role for CDCP1 as a unique HIF-2α target gene involved in the regulation of cancer metastasis and provide evidence that HIF-2α may be a critical factor promoting tumor metastasis in response to low oxygen. Further studies are warranted to characterize whether HIF-2α is sufficient to drive CDCP1-dependent metastasis in vivo and to determine whether CDCP1 expression correlates with metastasis or with a set of previously defined risk-stratification criteria for outcomes with metastatic ccRCC. Hypoxic tumors are commonly resistant to chemotherapy; therefore, targeting both the hypoxic response and CDCP1 with a monoclonal antibody may be an attractive strategy to control cancer progression, particularly metastasis.

Materials and Methods

Cell Lines, Cell Culture, and Virus Preparations. All cell lines were obtained from the American Type Culture Collection (ATCC), with the exception of the RCC cell lines A489, 786-0, and RCC4, which were provided by William G. Kaelin, Jr. (Dana-Farber Cancer Institute). 293T, DLD1, A375, A489, 786-0, and RCC4 were cultured in DMEM (Mediatech). HCT116 were cultured in McCoy's5A (ATCC). MCF10A were cultured in DMEM/F12 (Mediatech). Media were supplemented with 10% FBS (HyClone), 100 units/mL penicillin, 100 micrograms/mL streptomycin (Mediatech), and 20 mM Hepes (Mediatech). DMEM/F12 media for MCF10A were supplemented with 5% horse serum, 10 μg/mL insulin, 20 ng/mL EGF, 100 ng/mL cholera toxin, 0.5 μg/mL hydrocortisone, and 20 mM Hepes (Mediatech).

All cells were cultured in a humidified incubator at 37 °C/5% CO_2 unless otherwise stated. Hypoxic conditions (1% O_2) were obtained using a humidified variable aerobic workstation Invivo$_2$ 400 (Ruskinn). Deferoxamine was purchased from Sigma and dimethyloxaloylglycine was from Frontier Scientific. Retrovirus and lentivirus were produced in the 293T packaging cell line. Retroviral CDCP1 knockdown constructs were miR30-based RNAi constructs developed for the Hannon–Elledge libraries (3) and were obtained from Patrick Stern (Massachusetts Institute of Technology). The following hairpin oligonucleotides correspond to KD1 and KD2: KD1, 5′-TGCTGTTGACAGTGAGCGACCTGTTACATCGTCATTTCTATAGTGAAGCCACAGATGTATAGAAATGACGATGTAACAGGGTGCCTACTGCCTCGGA-3′, and KD2, 5′-TGCTGTTGACAGTGAGCGCCCTGAGAATCACTTTGTCATATAGTGAAGCCACAGATGTATATGACAAAGTGATTCTCAGGATGCCTACTGCCTCGGA-3′. Lentiviral infections were carried out as previously described (33). In brief, viruses were collected 48 h after infection, filtered, and used for infecting cells in the presence of 8 μg/mL polybrene before puromycin selection. All lentiviral vectors were obtained from the Broad Institute TRC shRNA library.

HIF-1α pLK0.1 shRNA sequence is TRCN0000003810; HIF-2α pLK0.1 shRNA sequence is TRCN0000003804 (1) and TRCN0000003805 (2); and ARNT pLK0.1 shRNA sequence is TRCN0000003819. The pLK0.1 empty vector and eGFP vector were used as controls. To generate virus using the above-described transfer vector, we used pMD2.G (Addgene; plasmid 12259) and psPAX2 (Addgene; plasmid 12260). Inducible cell lines were generated by infecting A375 cells with pMA2640 (Addgene; plasmid 25434), which encodes the rtTA gene. Next, cells were infected with virus encoding HA-HIF-2αDPA. HA-HIF-2αDPA was subcloned from Addgene plasmid 19006 to pLVX-tight-puro by adding NotI and an MluI site through PCR. All sequences were confirmed.

Immunoblot Analysis and Antibodies. Total cell lysates were prepared by washing cells with cold PBS, and then the cells were lysed with buffer

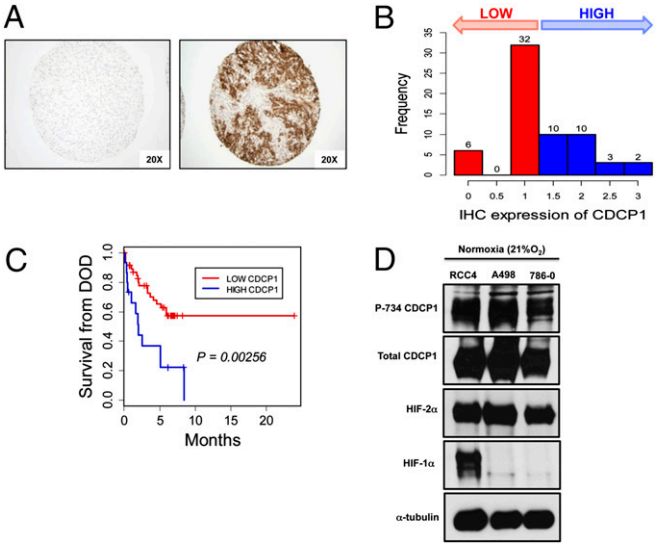

Fig. 4. High CDCP1 expression in ccRCC is associated with poor survival. Tissue microarray provided by the Kidney Cancer Tissue Acquisition, Pathology and Clinical Data Core Facility at The Dana-Farber Cancer Institute. The anti-CDCP1 antibody (Cell Signaling Technology) was used 1:500 with TSA. Pictures were taken under 20× magnification on a Leica microscope. (*A*) Representative pictures of total CDCP1 levels in RCC tumors (low and high expression of CDCP1, left to right). (*B*) Histogram of IHC expression of CDCP1. Numbers on top of the columns indicate the number of patients. (*C*) Kaplan–Meier survival analysis for patients with low vs. high CDCP1 expression. DOD, date of diagnosis. (*D*) Lysates from RCC cell lines (RCC4, A498, and 786-0) were immunoblotted for the phosphorylation (P-734) of CDCP1, total CDCP1, HIF-2α, and α-tubulin for loading control under normoxia (21% O_2).

containing 20 mM Tris·HCl (pH 7.5), 150 mM NaCl, 1 mM EDTA, 1 mM EGTA, and 1% Triton X-100, as well as protease and phosphatase inhibitors. Protein was measured using the Bradford assay (Bio-Rad), and at least 50 μg of total cell lysates was run on an SDS/polyacrylamide gel. The proteins were transferred onto a nitrocellulose membrane, and membranes were probed overnight at 4 °C with the appropriate primary antibody. Antibodies used were as follows: CDCP1, phosphotyrosine, Src, and phospho-Src family (Tyr416) (Cell Signaling Technology), HIF-1α and ARNT (BD Biosciences), α-tubulin (Sigma), and HA (Convance). The phospho-specific antibody against CDCP1 (Tyr734) was developed by Cell Signaling Technology. William G. Kaelin (Dana-Farber Cancer Institute) provided the HIF-2α antibody.

Immunoprecipitation. Cells were harvested and lysed as above. For immunoprecipitation experiments, cell lysates in 1% Triton X-100 lysis buffer were precleared with goat anti-mouse or anti-rabbit IgG agarose (Sigma) at 4 °C for 1 h. The precleared lysates were incubated with 1:100 diluted anti-CDCP1 antibody (Cell Signaling Technology) at 4 °C, and equal amounts of mouse or rabbit IgG (Santa Cruz Biotechnology) were used as controls. After overnight incubation, 20 μL of goat anti-mouse or anti-rabbit IgG agarose was added and incubated for an additional hour. The pellets were washed three times in 1% Triton X-100 lysis buffer and heated in 20 μL of 2× Laemmli buffer at 95 °C for 5 min, and the samples were run on 4–20% gradient SDS/polyacrylamide gels and probed with the indicated antibodies.

Transwell Migration Assays. Cells were serum-starved and exposed to 1% O_2 (37 °C) for 24 h before harvesting using PBS/EDTA, washed with serum-free media, and diluted to 1 × 10e5/mL in serum-free media. Five hundred microliters of media (with 10% serum) was added to the bottom of the transwell (8-μm pore; Costar) and 200 μL of cell suspension was added to the top of the filter. The plates were returned to 1% O_2 (37 °C) and, after 24 h, cells on top of the filter were removed using a cotton swab and the cells were fixed in formalin for 10 min before staining with 0.1% crystal violet for 30 min. The numbers of cells that had migrated to the bottom of the filter were counted. The CUB1 mAb (BioLegend) at 1 mg/mL was added at the time of seeding to the top and bottom chambers.

Quantitative Real-Time PCR. Total RNA was isolated from cells exposed to various conditions using the RNeasy Kit (Qiagen). qRT-PCR was performed at the Real Time PCR Core Facility(Beth Israel Deaconess Medical Center, BIDMC) using the Applied Biosystems TaqmanGene expression assay for CDCP1 (Hs01080405_m1). Cycle threshold values were normalized for amplification of 18S. The data presented are the results of triplicate analyses, and the error bars indicate SEM.

Chromatin Immunoprecipitation. ChIP assays were performed with the ChampionChIP Kit and protocol (SABiosciences). Briefly, MCF10A cells were grown at 21% O_2 (N) or 1% O_2 (H) for 48 h. Cells were fixed in 1% formaldehyde at room temperature for 10 min. Isolated nuclei were lysed followed by chromatin shearing. An anti–HIF-1α monoclonal antibody, anti–HIF-2α polyclonal antibody, and anti-ARNT polyclonal antibody (Novus Biologicals) were used. A mouse IgG antibody (Abcam) and rabbit IgG antibody (Abcam) were used as controls. After reverse cross-linking and DNA purification, DNA from input or immunoprecipitated samples was assayed with q-PCR. The following ChIP q-PCR assay was used to detect *Cdcp1* [GPH1022925(-)02A; SABiosciences]. DNA from input and immunoprecipitated samples was analyzed using the Light Cycler 480 II (Roche) with SYBR Green master mix (Bio-Rad). All cycle threshold (Ct) values were compared with the input amounts and to IgG controls to normalize for variations. The data were analyzed by using the Pfaffl method (34). The results were graphed as fold changes relative to specific background. Data are represented as the means ± SEM (n = 3).

Promoter Reporter Assay. Genomic human DNA (1.4 kb) surrounding the identified HIF binding site on chromosome 3 was cloned into the In-Fusion Ready Vector using the manufacturer's cloning protocol (Clontech) and subsequently cloned into the pLightSwitch_Prom reporter vector (SwitchGear Genomics). HT1080 cells were transfected and subjected to the conditions indicated. Luciferase assay was performed using the LightSwitch Luciferase assay reagents according to manufacturer's protocol (SwitchGear Genomics).

Xenografts. A volume of 200 μL of 1 × 10^6 tetracycline-inducible A375 cells (GFP or HIF-2αDPA) suspended in HBSS was injected into either flank of 7-wk-old NOD/SCID mice (Charles River). GFP vector control-expressing cells were injected on the left of the mouse and HIF-2αDPA–expressing cells were injected on the right side of the same mouse. Doxycycline treatment was performed by feeding animals 0.625 g/kg doxycycline (Rodent Diet 2018, 625 doxycycline; Harlan Laboratories). When tumors surpassed 2 mm, we measured them with calipers in two dimensions (L, length; W, width) two or three times a week. The average tumor volume was calculated as $V = L \times W^2 \times 0.52$. At the end of the experiment, the mice were euthanized and tumors were harvested and weighed. All animal care followed approved institutional guidelines of BIDMC. All animal experiments complied with National Institutes of Health guidelines and were approved by the BIDMC Animal Care and Use Committee.

Experimental Metastasis Assay. Six- to 8-wk-old NOD/SCID mice were injected via the lateral tail veins with A375 cells expressing the pBABE control or pBABE-HIF-2αWT (1× 10^6 cells) using a 30G needle. Ninety days later, mice were euthanized and lungs were inflated with 4% formalin in PBS, tied, and fixed for 5 min. Lungs were dissected and placed in ice-cold PBS and tumors were counted under a dissection microscope. All animal care followed approved institutional guidelines of BIDMC. All animal experiments complied with National Institutes of Health guidelines and were approved by the BIDMC Animal Care and Use Committee.

Immunohistochemistry. For CDCP1 IHC, 4-mm-thick sections were prepared from a formalin-fixed, paraffin-embedded tissue microarray block. Sections were deparaffinized, rehydrated, and heated with a pressure cooker to 125 °C for 30 s in citrate buffer for CDCP1 for antigen retrieval. After cooling to room temperature, sections were incubated in 3% hydrogen peroxide for 5 min to quench endogenous peroxidase (Dako). Sections were then incubated in avidin block for 15 min to quench endogenous avidin, followed by incubation in biotin block for 15 min to quench endogenous biotin (Vector Laboratories). The sections were then incubated with Protein Block Serum-Free (Dako) for 10 min. The primary antibody (CDCP1 antibody from Cell Signaling; 4115) was applied to sections for 1 h at a 1:500 dilution. Detection was performed by incubation with a Dako EnVision+ System HRP-labeled polymer (Dako; K4003 and K4001) for 30 min, followed by incubation with biotin-labeled tyramide (PerkinElmer; SAT700001EA) at a 1:50 dilution for 10 min. The slides were then incubated with LSAB2 streptavidin-HRP (Dako; K1016) for 30 min. DAB chromogen (Dako; K3468) was then

applied. Slides were slightly counterstained with hematoxylin. The specificity of the immunoassay was validated by staining FFPE cells that expressed stable shRNAs targeting CDCP1 (negative control) or the vector control shRNA (positive control) (Fig. S4).

Statistical Analysis. Bioinformatic analysis of CDCP1 was done as follows. Microarray expression data from six independent datasets (Fig. S3*A*) corresponding to tumor samples of different origins including bladder, breast (The Cancer Genome Atlas; http://tcga-data.nci.nih.gov/tcga), colon, kidney, ovarian, and pancreatic were downloaded from the Oncomine repository at www.oncomine.org to examine the relative mRNA expression levels of CDCP1 between normal and cancer samples. The distributions of log2 median-centered signal intensities were plotted using boxplots; differential gene expression was computed using the Welch two-sample *t* test, which is appropriate for subsets of unequal variances. Only the tumor sets that showed the same differential mode of expression in at least three independent datasets were included in this analysis. A heat map was generated to show that high CDCP1 expression (indicated in red) is a biomarker of poor prognosis in colon cancer (Fig. S3*B*). Tumors that showed 5-y recurrence had significantly higher CDCP1 mRNA levels ($P = 3.27 \times 10^{-4}$, Welch two-sample *t* test). A univariate Cox proportional hazard regression model was applied to correlate gene expression of CDCP1 with patient survival in a lung adenocarcinoma dataset of $n = 443$ samples; the likelihood ratio test, Wald test, and score (log-rank) test were all used to compute *P* values ($P < 1 \times 10^{-6}$ for all three tests). To visualize the result obtained from the survival analysis the samples were ranked according to CDCP1 gene expression, and Kaplan–Meier survival curves (Fig. S3*C*) were plotted for lung adenocarcinomas with the lowest (<25th percentile) versus highest (>25th percentile) CDCP1 expression, giving a *P* value of 8.1×10^{-7} (log-rank test).

The expression microarray data of the Sanger Cell Line Project (SCLP) ($n = 732$; cancer cell lines with mutation data of the common tumor suppressor genes and oncogenes) were downloaded from the Broad Institute server (www.broadinstitute.org), and a Pearson's correlation coefficient analysis was performed to correlate message levels of HIF-2α with CDCP1, as well as other known HIF-2α target genes, including MET and EGFR. *P* values were computed using an asymptotic confidence interval based on Fisher's Z transform, and the samples were clustered using the Euclidean distance metric and the complete linkage algorithm (Fig. 3 *D* and *E*).

All biological results are expressed as means of at least three or four independent experiments. Error bars represent the SEM. Statistical significance was determined by Student's *t* test (paired-data analysis). *P* values ≤0.05 (*) were considered to be statistically significant.

Human Tumor Samples and Data Analysis. Research involving human subjects was approved by The Dana-Farber/Harvard Cancer Center (DF/HCC) Institutional Review Board (IRB). Informed consent was obtained from all human subjects involved in research. Subjects participated in an IRB-approved protocol for tissue and data collection for use in clinical research. IHC analyses were performed on tissue samples from 63 deidentified subjects with ccRCC. Samples included patients with localized and metastatic disease.

ACKNOWLEDGMENTS. We thank William G. Kaelin for the HIF-2α antibody and for the RCC cell lines, Victoria Petkova for the qRT-PCR analysis (Real Time PCR Core, BIDMC), and the entire DF/HCC Kidney Cancer Specialized Programs of Research Excellence (SPORE) team. This work was supported by National Institutes of Health Grant 5R01GM056203-15 (to L.C.C.), American Cancer Society (ACS) Grant PF-08215-01-TBE, and a DF/HCC Career Development Award (to B.M.E.). G.P. is a Pfizer Fellow of the Life Sciences Research Foundation.

1. Rikova K, et al. (2007) Global survey of phosphotyrosine signaling identifies oncogenic kinases in lung cancer. *Cell* 131(6):1190–1203.
2. Scherl-Mostageer M, et al. (2001) Identification of a novel gene, CDCP1, overexpressed in human colorectal cancer. *Oncogene* 20(32):4402–4408.
3. Awakura Y, et al. (2008) Microarray-based identification of CUB-domain containing protein 1 as a potential prognostic marker in conventional renal cell carcinoma. *J Cancer Res Clin Oncol* 134(12):1363–1369.
4. Razorenova OV, et al. (2011) VHL loss in renal cell carcinoma leads to up-regulation of CUB domain-containing protein 1 to stimulate PKCdelta-driven migration. *Proc Natl Acad Sci USA* 108(5):1931–1936.
5. Hooper JD, et al. (2003) Subtractive immunization using highly metastatic human tumor cells identifies SIMA135/CDCP1, a 135 kDa cell surface phosphorylated glycoprotein antigen. *Oncogene* 22(12):1783–1794.
6. Perry SE, et al. (2007) Expression of the CUB domain containing protein 1 (CDCP1) gene in colorectal tumour cells. *FEBS Lett* 581(6):1137–1142.
7. Miyazawa Y, et al. (2010) CUB domain-containing protein 1, a prognostic factor for human pancreatic cancers, promotes cell migration and extracellular matrix degradation. *Cancer Res* 70(12):5136–5146.
8. Bhatt AS, Erdjument-Bromage H, Tempst P, Craik CS, Moasser MM (2005) Adhesion signaling by a novel mitotic substrate of src kinases. *Oncogene* 24(34):5333–5343.
9. Spassov DS, Baehner FL, Wong CH, McDonough S, Moasser MM (2009) The transmembrane src substrate Trask is an epithelial protein that signals during anchorage deprivation. *Am J Pathol* 174(5):1756–1765.
10. Uekita T, et al. (2007) CUB domain-containing protein 1 is a novel regulator of anoikis resistance in lung adenocarcinoma. *Mol Cell Biol* 27(21):7649–7660.
11. Uekita T, et al. (2008) CUB-domain-containing protein 1 regulates peritoneal dissemination of gastric scirrhous carcinoma. *Am J Pathol* 172(6):1729–1739.
12. Ikeda J, et al. (2009) Expression of CUB domain containing protein (CDCP1) is correlated with prognosis and survival of patients with adenocarcinoma of lung. *Cancer Sci* 100(3):429–433.
13. Deryugina EI, et al. (2009) Functional role of cell surface CUB domain-containing protein 1 in tumor cell dissemination. *Mol Cancer Res* 7(8):1197–1211.
14. Fukuchi K, et al. (2010) Inhibition of tumor metastasis: Functional immune modulation of the CUB domain containing protein 1. *Mol Pharm* 7(1):245–253.
15. Benes CH, et al. (2005) The C2 domain of PKCdelta is a phosphotyrosine binding domain. *Cell* 121(2):271–280.
16. Liu H, et al. (2011) CUB-domain-containing protein 1 (CDCP1) activates Src to promote melanoma metastasis. *Proc Natl Acad Sci USA* 108(4):1379–1384.
17. Ivan M, et al. (2001) HIFalpha targeted for VHL-mediated destruction by proline hydroxylation: Implications for O_2 sensing. *Science* 292(5516):464–468.
18. Jaakkola P, et al. (2001) Targeting of HIF-alpha to the von Hippel-Lindau ubiquitylation complex by O_2-regulated prolyl hydroxylation. *Science* 292(5516):468–472.
19. Bell EL, et al. (2007) The Qo site of the mitochondrial complex III is required for the transduction of hypoxic signaling via reactive oxygen species production. *J Cell Biol* 177(6):1029–1036.
20. Wang GL, Jiang BH, Rue EA, Semenza GL (1995) Hypoxia-inducible factor 1 is a basic-helix-loop-helix-PAS heterodimer regulated by cellular O_2 tension. *Proc Natl Acad Sci USA* 92(12):5510–5514.
21. Semenza GL (2003) Targeting HIF-1 for cancer therapy. *Nat Rev Cancer* 3(10):721–732.
22. Gordan JD, Simon MC (2007) Hypoxia-inducible factors: Central regulators of the tumor phenotype. *Curr Opin Genet Dev* 17(1):71–77.
23. Raval RR, et al. (2005) Contrasting properties of hypoxia-inducible factor 1 (HIF-1) and HIF-2 in von Hippel-Lindau-associated renal cell carcinoma. *Mol Cell Biol* 25(13):5675–5686.
24. Kondo K, Klco J, Nakamura E, Lechpammer M, Kaelin WG, Jr. (2002) Inhibition of HIF is necessary for tumor suppression by the von Hippel-Lindau protein. *Cancer Cell* 1(3):237–246.
25. Maranchie JK, et al. (2002) The contribution of VHL substrate binding and HIF1-alpha to the phenotype of VHL loss in renal cell carcinoma. *Cancer Cell* 1(3):247–255.
26. Kondo K, Kim WY, Lechpammer M, Kaelin WG, Jr. (2003) Inhibition of HIF2alpha is sufficient to suppress pVHL-defective tumor growth. *PLoS Biol* 1(3):E83.
27. Zimmer M, Doucette D, Siddiqui N, Iliopoulos O (2004) Inhibition of hypoxia-inducible factor is sufficient for growth suppression of VHL–/– tumors. *Mol Cancer Res* 2(2):89–95.
28. Shen C, et al. (2011) Genetic and functional studies implicate HIF1α as a 14q kidney cancer suppressor gene. *Cancer Discov* 1(3):222–235.
29. He Y, et al. (2010) Proteolysis-induced N-terminal ectodomain shedding of the integral membrane glycoprotein CUB domain-containing protein 1 (CDCP1) is accompanied by tyrosine phosphorylation of its C-terminal domain and recruitment of Src and PKCdelta. *J Biol Chem* 285(34):26162–26173.
30. Benes CH, Poulogiannis G, Cantley LC, Soltoff SP (2012) The SRC-associated protein CUB domain-containing protein-1 regulates adhesion and motility. *Oncogene* 31(5):653–663.
31. Bruick RK, McKnight SL (2001) A conserved family of prolyl-4-hydroxylases that modify HIF. *Science* 294(5545):1337–1340.
32. Epstein AC, et al. (2001) *C. elegans* EGL-9 and mammalian homologs define a family of dioxygenases that regulate HIF by prolyl hydroxylation. *Cell* 107(1):43–54.
33. Moffat J, et al. (2006) A lentiviral RNAi library for human and mouse genes applied to an arrayed viral high-content screen. *Cell* 124(6):1283–1298.
34. Pfaffl MW (2001) A new mathematical model for relative quantification in real-time RT–PCR. *Nucleic Acids Res* 29(9):e45, 10.1093/nar/29.9.e45.